β-TCP-FeMg biodegradable nanocomposites: *in vivo* behavior and bone scaffold processing

S.K. Swain[1], I. Gotman[1], and E.Y. Gutmanas[1,2]*

[1] Department of Materials Science and Engineering, Technion-Israel Institute of Technology, Haifa, 32000, Israel
[2] Tomsk Polytechnic University, Tomsk, 634050, Russia

40 to 70% porous beta-tricalcium phosphate (β-TCP) based bone scaffolds reinforced by FeMg metallic phase were produced by mixing precompacted nanocomposite granules (β-TCP with 30 vol % FeMg) of different size with salt particles followed by high pressure consolidation at room temperature and porogen dissolution. The use of precompacted granules instead of the loose β-TCP-30 (FeMg) powder allowed us to obtain scaffolds with high Darcy's permeability while maintaining load bearing characteristics. Scaffolds with 50% porosity exhibited the best combination of compressive strength (8.5–10.5 MPa) and permeability (~3.5×10^{-10} m^2) falling within the range of trabecular bone. Subcutaneous implantation of dense β-TCP-30 (FeMg) discs in mice demonstrated the absence of the scaffold material toxicity. The formation of degradation products (Fe-oxides and Fe-phosphate) on the implant surface, as well as a 30–40 % loss of compressive strength after 3 months implantation indicated the degradation of β-TCP-30 (FeMg) *in vivo*. No pronounced reduction in volume or mass loss was observed suggesting the protective action of the iron-phosphate surface layer.

Keywords: bone scaffold, nanocomposite, β-TCP, iron, magnesium, subcutaneous implantation

1. Introduction

The requirement for new bone to replace or restore the function of damaged or lost bone is a major clinical and socioeconomic need. To facilitate bone regeneration under sub-optimal conditions, bone supplementation is often needed. Bone supplementation is usually accomplished with autologous bone which, however, is not always available in sufficient amounts and whose harvesting imposes health concerns, e.g. donor site morbidity [1–3]. Bone allografts are inferior to autologous bone as they fail to supply osteogenic cells and, in addition, have known risks of bacterial contamination, viral transmission and immunogenicity [1, 3–5]. The above limitations of conventional bone grafts have initiated the search for a dependable synthetic bone graft substitute.

A bone graft substitute is placed into the defect to help maintain space and to act as a scaffold for bone tissue regeneration. The scaffold should be highly porous with interpenetrating pore structure to allow for the transport of body fluids, bone cells and endothelial cells which form the vasculature supplying the bone with oxygen and nutrients [1, 6]. The pore size must be within a critical range, typically 100–400 μm [7, 8]. The choice of a suitable material is paramount as the scaffold has to be osteoconductive, i.e. to possess the right surface chemistry to allow for attachment and inward migration of bone cells and, at the same time, should possess appropriate mechanical properties to provide the correct stress environment for the new bone formation and to withstand *in vivo* loads. The latter requirement is especially challenging since it is difficult to maintain high strength with high porosity. Ideally, the scaffold must also be biodegradable, with non-toxic byproducts, and disappear from the site when tissue regeneration is completed. This will allow for a gradual transfer of mechanical loads to the forming bone and prevent adverse effects on the host, such as stress shielding-related bone loss and long-term foreign body reaction.

Various porous materials have been considered as bone graft substitutes: ceramics, polymers, metals, and composites. Degradable polymers such as polylactic and polyglycolic acids and their copolymers (PLA, PGA and PLGA) exhibit attractive degradation patterns but are weak, lack osteoconductivity and degrade to acidic products that can

* *Corresponding author*
Prof. Elazar Y. Gutmanas, email: gutmanas@tx.technion.ac.il

cause late inflammation and osteolysis in bone contact [9]. Resorbable Ca phosphate (CaP) ceramics (tricalcium phosphate (TCP), Ca-deficient hydroxyapatite, (HA)) are osteoconductive due to the close resemblance to the bone mineral, however they are intrinsically brittle and thus unsuitable for use on their own in load-bearing sites [4, 10]. Combining degradable polymers with CaP ceramics has been shown to produce bioresorbable composite materials with improved mechanical properties [11, 12]. Notably, Ca-deficient HA and β-TCP matrix composites with 20–40 vol % uniformly distributed PLA or PCL polymer produced by high pressure consolidation of powders exhibited an attractive combination of compressive strength, flexural strength and ductility [13–16]. 50% porous β-TCP-40PLA composite scaffolds were reported to possess an attractive combination of compressive strength and pore interconnectivity falling within the range of trabecular bone [17]. Still, the strength of these polymer-toughened CaPs is limited by the low strength of the polymer component. Toughening CaP ceramics with biodegradable metals (such as magnesium and iron) that are significantly stronger than polymers can potentially produce composite biomaterials and porous scaffolds with enhance mechanical properties. Magnesium is light and has a relatively low elastic modulus approaching that of the cortical bone. However, the corrosion of magnesium in physiological conditions is too fast and is accompanied by the evolution of hydrogen and formation of gas bubbles that can cause adverse reactions and inhibit bone growth [18, 19]. Iron is stronger than magnesium and probably more suitable for load-bearing bone healing, but its degradation in the physiological conditions is too slow for most implant applications [20, 21]. A uniform mixture of nanoscale Fe and Mg is expected to corrode at a rate intermediate between iron and magnesium thus to act as an appropriate metallic reinforcement for β-TCP-based biomaterials and bone scaffolds. Recently, we've reported that dense β-TCP nanocomposites reinforced with 30 vol % iron-magnesium metallic phase exhibited high compressive and bending strength, attractive strength degradation behavior in aqueous media and *in vitro* cell compatibility [22]. In the present paper, *in vivo* degradation and toxicity of the β-TCP-FeMg nanocomposites are examined and the fabrication and properties of porous β-TCP-FeMg scaffolds are reported.

2. Experimental

2.1. Fabrication and characterization of β-TCP-FeMg scaffolds

β-tricalcium phosphate (β-TCP, $Ca_3(PO_4)_2$) nanopowder (100–200 nm) was prepared by chemical precipitation method using calcium nitrate tetrahydrate ($Ca(NO_3)\cdot 4H_2O$), phosphoric acid (H_3PO_4) and 25% ammonia solution (NH_4OH), as described in [16]. In brief, 0.5 M $Ca(NO_3)\cdot 4H_2O$ and H_3PO_4 were mixed with 1.5 : 1 Ca-to-P atomic ratio and poured into a large excess of NH_4OH. The obtained precipitate was rinsed with water, boiled for 30 min in a microwave oven, vacuum dried and calcined at 700°C for 24 h.

50Fe–50Mg metal powder blends were prepared from carbonyl Fe powder (~2 μm) and Mg powder (<40 μm) as described in [22]. The powders were mixed and high energy attrition milled (Union Process 01HD) at 800 rpm in hexane under argon atmosphere for 4 h, with balls (stainless steel, 4 mm)-to-powder ratio of 20 : 1. 30 vol % of the prepared 50Fe50Mg blend was mixed with 70 vol % β-TCP powder and attrition milled for 4 h under the same conditions as above to yield a β-TCP–15Fe15Mg composition.

Macroporous β-TCP-15Fe15Mg composite scaffolds with 40 to 70% porosity were prepared employing the modified salt leaching method [17]. β-TCP-15Fe15Mg nanocomposite powder was pre-compacted at 400 MPa to 18 mm diameter disks, crushed in a mortar to produce granules that were sieved to two different sizes: 100–200 and 200–300 μm. Sodium sulphate (Na_2SO_4) porogen particles (200–800 μm) were crushed and sieved to the 100–200 and 200–300 μm fractions. The β-TCP–15Fe15Mg granules were mixed with the porogen particles of the same size and high pressure consolidated/cold sintered at 2.5 GPa. The porogen was then removed by rinsing in DI water. The final dimensions of scaffolds obtained were 11mm diameter and 3mm thickness. The rationale behind using granules of the matrix material (instead of the loose powder) with the size comparable to that of the porogen is to prevent "encapsulation" of the relatively large (typically 100–500 μm) porogen particles by the matrix. This significantly increases the contact area between the porogen particles (before leaching) and generates high pore interconnectivity after porogen leaching [17].

The architecture and pore structure of the scaffolds was examined in a scanning electron microscope, SEM (FEI Quanta 200). To study the microstructure of the scaffold struts, the scaffolds were broken in bending and the fracture surfaces observed in SEM and in a high resolution SEM, HRSEM (Zeiss Ultra Plus). The scaffolds compressive strength was measured in an 1195 Instron testing machine at the strain rate 10^{-5} s^{-1}. At least three scaffolds of each type were tested.

The scaffold permeability, k (m^2) was measured in a homemade falling-head permeameter using ethanol as the flowing fluid. The method is based on Darcy's law of flow through porous media:

$$Q\frac{L}{A}=\frac{k}{\mu}\Delta P,$$

where Q is the flow rate, L and A are scaffold length and cross-sectional area respectively, μ is the fluid viscosity (1.2×10^{-3} Pa×s for ethanol) and ΔP is the pressure drop across the scaffold. The test consisted of measuring the time

required for the head to drop through a known distance. The calculated flow rate was plotted against pressure drop, and the permeability was determined from the slope of the straight line obtained [23]. All the measurements were performed in triplicate on at least three scaffolds of each type.

2.2. In vivo testing of toxicity and biodegradability of β-TCP-FeMg composites

In vivo toxicity of βTCP-FeMg nanocomposites was assessed in a murine subcutaneous model. All experimental procedures for the study were conducted in compliance with animal welfare regulations of the Israeli Ministry of Health as approved by the Technion animal care committee. Twenty two-month old male mice were housed under controlled conditions and fed a standard pellet diet and water ad libitum. The mice were divided into 5 groups of four animals: one control group, two groups with TCP15Fe15Mg implants and two groups with β-TCP24Fe6Mg implants. Mice in all but control groups were anaesthetized by intraperitoneal injection of 100 mg/kg of ketamine and 10 mg/kg of xylazine. The back of each mouse was shaved and disinfected and a small skin incision was made through the full thickness of the skin. Subcutaneous pockets between the fascia of the dorsal muscles and the subcutaneous tissue were created on one side of the back by blunt dissection with scissors. β-TCP-15Fe15Mg and β-TCP-24Fe6Mg discs with 3 mm diameter, 1.4 mm thickness and 95–96% relative density were prepared by high pressure consolidation (cold sintering) of the corresponding attrition milled powders blends at 2.5 GPa [22]. One β-TCP-FeMg disc was inserted into each subcutaneous pocket and the incisions were closed by surgical staples. All the groups of mice were observed and weighed regularly. After one month and 3 months of observation, the animals were killed by an injection of pentobarbitone sodium. The implants with surrounding tissue were harvested, carefully separated from the tissue, cleaned and air-dried. The implants were then examined in SEM and their surface composition analyzed by Energy Dispersive Analysis (EDS). The excised β-TCPFeMg discs were tested in compression (in an 1195 Instron machine) and their strength compared with that of the corresponding as-prepared discs.

To evaluate systemic toxicity, complete blood cell count (white blood cell, red blood cell, thrombocyte) was performed on 2 mice from control group and on 2 mice from each 3-months group on day 30, 55 and day 80. Corrosion products are known to accumulate in and be cleared by the mononuclear phagocyte system organs (spleen and liver). We, therefore, analyzed the effect of the implanted materials on the spleen and liver. These organs were excised from all killed animals and their weights were measured.

3. Results

3.1. β-TCP-15Fe15Mg scaffold properties

In Fig. 1, representative micrographs of macroporous βTCP-15Fe15Mg scaffolds are shown. Depending on the porogen used, the pore size ranges between 90–220 μm (Fig. 1a) or 120–300 μm (Fig. 1b). Both values fall within the suggested optimal pore size of bone scaffolds. Moreover, the pores are not isolated but form interconnected channels—a critical requirement for blood vessel formation needed for successful bone ingrowth. Even the most porous scaffolds were mechanically robust and did not break when handled.

The microstructure of the scaffold struts (fracture surface) is shown in Fig. 2. It can be seen that the struts are dense and consist of submicron/several micron size metallic regions (bright) uniformly distributed within the largely ceramic β-TCP matrix (Fig. 2a). This is very similar to the microstructure of dense cold sintered β-TCP-15Fe15Mg composites reported in [22]. At high magnifications (Fig. 2b), fine 100–200 nm particles of β-TCP with occasional nanoscale metallic inclusions can be seen, also comparable with the observations in [22]. In that paper it has been shown that the β-TCP matrix contains a few percent of Mg distrib-

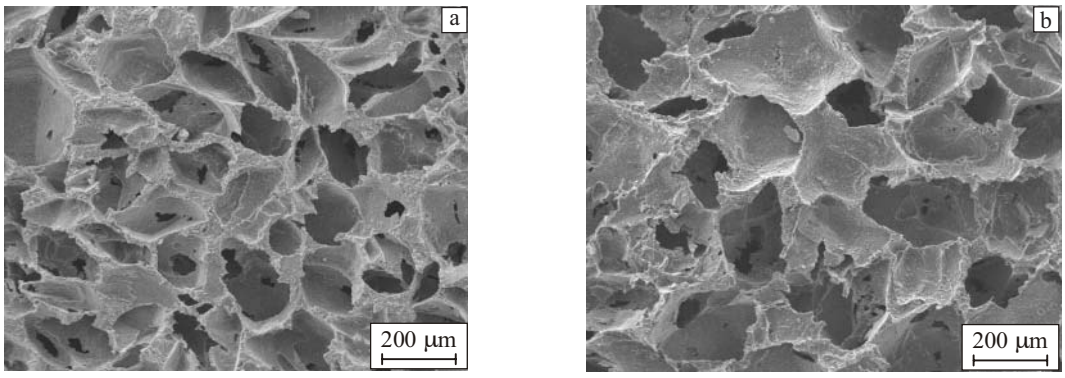

Fig. 1. Macroporous β-TCP-15Fe15Mg scaffolds produced by the modified salt leaching method: 60% porosity, 100–200 μm granules (a); 70% porosity, 200–300 μm granules (b). SEM.

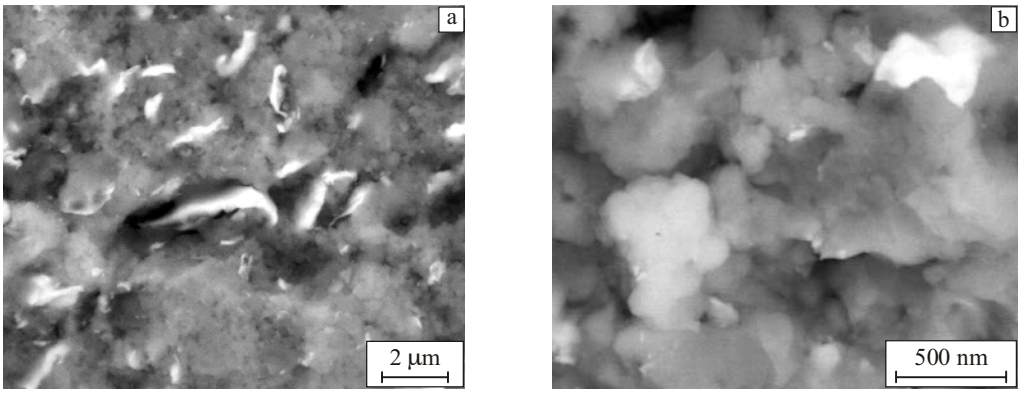

Fig. 2. Representative microstructure of the β-TCP-15Fe15Mg scaffold struts. Fracture surfaces: SEM (a), high resolution SEM (b).

uted as a very thin layer between the β-TCP nanoparticles. This ductile metallic layer acts a "glue" and promotes room temperature consolidation of the ceramic particles into a dense monolithic material.

Figure 3 shows the compressive strength σ_c, and Darcy's permeability k, of β-TCP-15Fe15Mg scaffolds as a function of density and granule size. The comparison of the β-TCP-FeMg scaffolds with the β-TCP-PLA scaffolds prepared by the same procedure of attrition milling, cold sintering and modified salt leaching [17] shows that, for the same macroporosity, the metal-reinforced scaffolds are measurably more permeable than the polymer-based ones. For example, the highest permeability value reported for 50%-porous β-TCP-40PLA scaffolds was 1.5×10^{-10} m^2—more than twice lower than for the corresponding β-TCP-15Fe15Mg scaffolds ($3.0–3.5\times10^{-10}$ m^2). Furthermore, at the same permeability (e.g. 0.3×10^{-10} m^2) the metal-reinforced scaffolds are significantly stronger than the polymer-based ones (17–18 versus 4–5 MPa). As seen in representative stress-strain curves in Fig. 4, the 40 and 50% porous β-TCP-15Fe15Mg scaffolds withstand a small but measurable amount of plastic strain ($0.5\% < \varepsilon_p < 1\%$) before fracture. This is a clear improvement over the literature reported pure calcium phosphate (HA, β-TCP) scaffolds that fail catastrophically in compression with no apparent plastic deformation [24–26]. The elastic moduli (E) of the 40 and 50% porous β-TCP-15Fe15Mg scaffolds calculated from the slopes of the corresponding stress-strain curves are 1.0 GPa and 400 MPa, respectively. Both the moduli and the strengths of these scaffolds are comparable with the corresponding values reported for human tibial trabecular bone, ranging from 200 to 900 MPa for Young's modulus, and from 5.3 to 9.5 MPa for ultimate stress in compression [27]. On the whole, 50–55% porous β-TCP-15Fe15Mg scaffolds definitely fall within the range of trabecular bone in terms of elastic modulus, strength and permeability [27–34]. Further optimization of granule/porogen size and processing parameters (compaction/consolidation pressure-temperature, heat treatment) will allow us to fabricate scaffolds with an even better combination of properties.

3.2. In vivo study of β-TCP-FeMg material

All mice were healthy throughout the experiment and showed no changes in physical appearance or activity due to implantation. Blood count levels were similar for the treated and control animals. The tested organs of the implanted mice did not show any abnormal gross weight

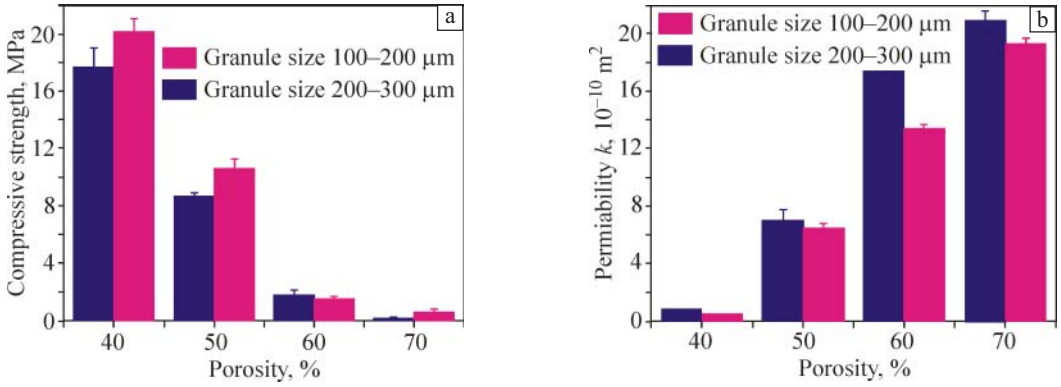

Fig. 3. Compressive strength (a) and Darcy's permeability k (b) of β-TCP-15Fe15Mg scaffolds as a function of porosity and granule size.

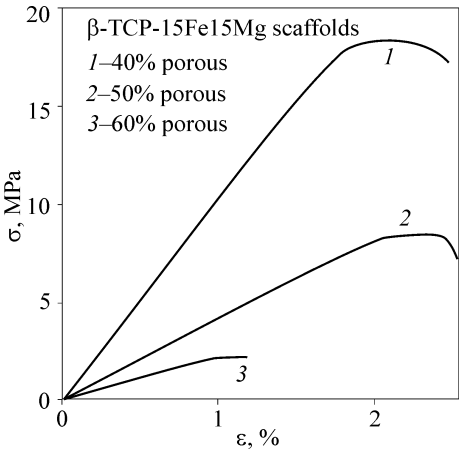

Fig. 4. Stress-strain curves in compression of β-TCP-15Fe15Mg scaffolds of different porosities produced from matrix granules 200–300 μm in size.

changes compared to the control group. Visual inspection of the implant site revealed no evidence of acute inflammation or tumor formation associated with the implant, only the formation of fibrous tissue around the implant. These results suggest the absence of systemic toxicity of the developed β-TCP-FeMg composites and their corrosion/degradation products in the mouse model. It is worth mentioning that in our recent publication, the β-TCP-15Fe15Mg composite was shown to support the attachment and proliferation of osteoblast and endothelial cells and the cells exhibited characteristic markers for bone formation and angiogenesis, respectively [22].

After 3 months implantation, the β-TCP-FeMg composite discs retained their shape and integrity. This is clearly illustrated by Fig. 5a. No pronounced reduction in volume or mass change were measured. The majority of implants gained a few percent weight, most probably due to small fragments of tissue remaining on the implant, or as a result of corrosion products formation. As can be seen in Fig. 5b, a uniform layer of degradation products covered the surface of the discs. According to the EDS analysis, the degradation product layer contained all the component elements of β-TCP-FeMg, as well as other elements that originate from the living organism, i.e. Na and K. The amount of iron (relative to magnesium) in this surface layer was much higher than in the corresponding Fe-Mg phase prior to implantation. Regardless of the starting composition, the Fe-to-Mg atomic ratio on the surface ranged from 7 : 1 to 15 : 1 versus 1 : 1 in β-TCP-15Fe15Mg or 4 : 1 in β-TCP-24Fe6Mg. Apparently, the surface of the implanted composites was depleted of Mg due to the more rapid corrosion of Mg accelerated by the presence of the more noble Fe metal acting as a cathode. The EDS atomic ratios of P-to-Ca and oxygen-to-Ca measured on the surface of excised β-TCP-FeMg implants were substantially higher than those of the β-TCP ($Ca_3(PO_4)_2$) component: (1.2–1.4) versus 0.67 and (5–6) versus 2.67, correspondingly. This implies that the degradation product layer consists of iron oxides/hydroxides and iron phosphate. *In vivo* formation of iron phosphate on biodegradable iron implants has been recently reported by other researchers, both in a subcutaneous mouse model [35], and in a rat transcortical femur model [36]. It has been suggested in [36] that precipitation of iron phosphate (formed by reaction of the dissolved Fe ions with the phosphate ions of the body fluids) is caused by the local rise of pH due to generation of OH^- by oxygen reduction. The dense layer of insoluble degradation products hinders the transport of oxygen towards the implant surface. As dissolved oxygen is necessary for appreciable corrosion of Fe in the near-neutral body environment [37] the implant degradation rate is strongly reduced.

The very small, if any, amount of mass loss after 3 months implies that no significant bioresorption of the β-TCP component took place during subcutaneous implantation of the β-TCP-FeMg discs. β-TCP is considered bioresorbable (much more than HA) and is known to promote new bone formation directly on the implant surface [10]. However, the reports on the *in vivo* resorption rate of β-TCP are contradictory. Gradual dissolution was reported

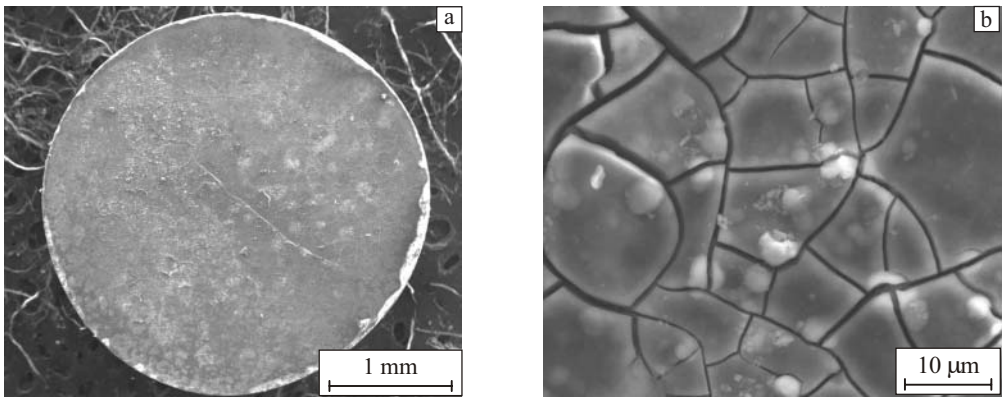

Fig. 5. Dense β-TCP-15Fe15Mg disc excised after 3 months murine subcutaneous implantation.

for 250–500 μm β-TCP granules placed in cranial defects of rats with only 23% of the implant volume remaining after 6 months implantation [38]. The remaining β-TCP was directly in contact with the newly formed bone. In another research, in contrast, 150–500 μm β-TCP granules implanted in the calvaria of rats were clearly visible without any alterations regarding their size and shape six months after surgery [39]. β-TCP implants were surrounded by a thin fibrous layer with no presence of osteoblasts and features of regular mineralization. It has been suggested by many authors that *in vivo*, the resorption of β-TCP occurs through the combined action of cell-mediated degradation and physicochemical dissolution [10, 40]. The β-TCP compound has low water solubility at the near-neutral pH typical of the body fluids. Thus, both suggested resorption mechanisms are believed to be mediated by a local drop in pH, caused either by osteoclast secretion of H^+ or by acidic by-products of metabolic activity of differentiating osteogenic cells [41–43]. Whatever the case, the subcutaneous environment is lacking the cellular characteristics of bone and thus does not provide factors essential for bioresorption of β-TCP. It was reported, for example, that tricalcium phosphate implants consisting of a mixture of α- and β-TCP were bioactive, biodegradable and osteoconductive in rat tibiae however showed no signs of resorption after 120 days implantation in rat subcutaneous tissue [44].

Despite the absence of visible *in vivo* degradation of the β-TCP-FeMg implants, a significant loss of compressive strength was measured after 3 months implantation: from 420±17 MPa to 239±41 MPa (43%) for β-TCP-15Fe15Mg, and from 270±12 MPa to 195±26 MPa (28%) for β-TCP-24Fe6Mg. The observed change in strength confirms the resorbability of the developed composite material. A similar degradation behavior—a pronounced (> 50%) loss of bending strength after one month with minimal concomitant weight change (±3%) was reported for dense cold sintered β-TCP-FeMg nanocomposites immersed in Ringer's solution [22]. The significant strength degradation not accompanied by the apparent material loss can be explained by the localized material dissolution concentrated at the interfaces between the β-TCP grains and the metallic phase. As described above, a thin magnesium layer bonding together the β-TCP nanoparticles is responsible for the high initial strength of the cold sintered β-TCP-FeMg nanocomposites. The corrosion of this interconnected Mg network weakens the bonding between the β-TCP particles and leads to the loss of strength. Furthermore, the mechanical strength loss may be caused by the dissolution of some β-TCP grain surfaces due to the possible water penetration along the corroded Mg network and through the micro- or nanopores of the 95–96% dense β-TCP-FeMg implants. This latter mechanism was proposed as an explanation for the compressive strength loss, from 419 to 158 MPa (62%), not accompanied by any significant weight change, of 96% dense high-temperature sintered β-TCP samples upon 16 weeks immersion in SBF solution [45]. A similar strength degradation trend accompanied by only marginal weight change was reported for 92.5% dense β-TCP discs immersed in SBF for 8 weeks [46].

4. Conclusions

Porous β-tricalcium phosphate-based nanocomposite scaffolds for bone tissue regeneration reinforced with 30 vol % biodegradable Fe-Mg metal phase were manufactured by a combination of high pressure consolidation and a modified particulate leaching method. Due to the use of precompacted matrix granules instead of the loose β-TCP-metal powder, the scaffolds possessed high pore interconnectivity/permeability, on a par with the trabecular bone. The best combination of permeability and load bearing characteristics was obtained for scaffolds with 50–55% porosity. At the same permeability, the metal-reinforced β-TCP-FeMg scaffolds were significantly stronger than the earlier reported similarly processed polymer-toughened β-TCP-PLA scaffolds.

Subcutaneous implantation studies of dense β-TCP-FeMg scaffold materials in a mouse model demonstrated no post-operative signs of toxicity and no clinical abnormalities. Formation of degradation products (Fe-oxides and Fe-phosphate) on the implant surface was clearly observed, however no pronounced reduction in volume or mass loss was apparent. A 30–40 % loss of compressive strength was measured after 3 months implantation demonstrating that *in vivo* degradation of the investigated materials took place. The possible inhibition of β-TCP-FeMg corrosion by the iron-phosphate passivation layer, as well as strategies to control the *in vivo* degradation rates should be further investigated.

Acknowledgments

This work was supported by Israel Science Foundation-ISF through research grant No. 1326/11.

References

1. Ilan DI, Ladd AL. Bone graft substitutes. Oper Tech Plast Reconstr Surg. 2003; 9: 151–160.
2. St John TA, Vaccaro AR, Sah AP, Schaefer M, Berta SC, et al. Physical and monetary costs associated with autogenous bone graft harvesting. Am J Orthop. 2003; 32: 18–23.
3. Ducheyne P, Qiu Q. Bioactive ceramics: the effect of surface reactivity on bone formation and bone cell function. Biomater. 1999; 20: 2287–303.
4. Johnson KD, Frierson KE, Keller TS, Cook C, Scheinberg R, et al. Porous ceramics as bone graft substitutes in long bone defects: a biomechanical, histological, and radiographic analysis. J Orthop Res. 1996; 14: 351–69.
5. Vaccaro AR, Cirello J. The use of allograft bone and cages in fractures of the cervical, thoracic, and lumbar spine. Clin Orthop Rel Res. 2002; 394: 19–26.

6. Bauer TW, Muschler GF. Bone graft materials: an overview of the basic science. Clin Orthop Rel Res. 2000; 371: 10–27.
7. Bobyn JD, Pilliar RM, Cameron HU, Weatherly GC. The optimum pore size for the fixation of porous surfaced metal implants by the ingrowth of bone. Clin Orthop Rel Res. 1980; 150: 263–269.
8. Karageorgiou V, Kaplan D. Porosity of 3D biomaterial scaffolds and osteogenesis. Biomaterials. 2005; 26: 5474–5491.
9. Sung H-J, Meredith C, Johnson C, Galis ZS. The effect of scaffold degradation rate on three-dimensional cell growth and angiogenesis. Biomaterials. 2004; 25: 5735–5742.
10. Bohner M. Calcium orthophosphates in medicine: from ceramics to calcium phosphate cements. Injury. 2000; 31: SD37–47.
11. Ignjatović N, Suljovrujic E, Budinski-Simendic J, Krakovsky I, Uskoković DP. Evaluation of hot-pressed hydroxyapatite/poly-L-lactide composite biomaterial characteristics. J Biomed Mater Res B. 2004; 71B: 284–294.
12. Kikuchi M, Koyama Y, Yamada T, Imamura Y, Okada T, et al. Development of guided bone regeneration membrane composed of beta-tricalcium phosphate and poly (L-lactide-co-glycolide-co-epsilon-caprolactone) composites. Biomaterials. 2004; 25: 5979–5986.
13. Bernstein M, Gotman I, Makarov C, Phadke A, Radin S, Ducheyne P, Gutmanas EY. Low temperature fabrication of β-TCP-PCL nanocomposites for bone implants. Adv Eng Mater. 2010; 12(8): B341–B347.
14. Makarov C, Gotman I, Jiang X, Fuchs S, Kirkpatrick CJ, Gutmanas EY. In situ synthesis of calcium phosphate-polycaprolactone nanocomposites with high ceramic volume fractions. J Mater Sci: Mater Med. 2010; 21: 1771–1779.
15. Rakovsky A, Gotman I, Rabkin E, Gutmanas EY. Strong bioresorbable Ca phosphate-PLA nanocomposites with uniform phase distribution by attrition milling and high pressure consolidation. J Mech Behav Biomed Mater. 2013; 18: 37–46.
16. Makarov C, Berdicevsky I, Raz-Pasteur A, Gotman I. *In vitro* antimicrobabial activity of vancomycin-eluting bioresorbable β-TCP-polylactic acid nanocomposite material for load-bearing bone repair. J Mater Sci: Mater Med. 2013; 24: 679–687.
17. Rakovsky A, Gotman I, Rabkin E, Gutmanas EY. β-TCP-polylactide composite scaffolds with high strength and enhanced permeability prepared by a modified salt leaching method. J Mech Behav Biomed Mater. 2014; 32: 89–98.
18. Martinez Sanchez AH, Luthringer BJC, Feyerabend F, Willumeit R. Mg and Mg alloys: How comparable are *in vitro* and *in vivo* corrosion rates? Rev Acta Biomater. 2015; 13: 16–31.
19. Staiger MP, Pietak AM, Huadmai J, Dias G. Magnesium and its alloys as orthopedic biomaterials. Rev Biomater. 2006; 27: 1728–1734.
20. Hermawan H, Purnama A, Dube D, Couet J, Mantovani D. Fe-Mn alloys for metallic biodegradable stents: Degradation and cell viability studies. Acta Biomater. 2010; 6: 1852–1860.
21. Schinhammer M, Hänzi AC, Löffler JF, Uggowitzer PJ. Design strategy for biodegradable Fe-based alloys for medical applications. Acta Biomater. 2010; 6: 1705–1713.
22. Swain SK, Gotman I, Unger R, Kirkpatrick CJ, Gutmanas EY. Microstructure, mechanical characteristics and cell compatibility of â-tricalcium phosphate reinforced with biodegradable Fe-Mg metal phase. J Mech Behav Biomed Mater. 2016; 53: 434–444.
23. Li S, De Wijn JR, Li J, Layrolle P, De Groot K. Macroporous biphasic calcium phosphate scaffold with high permeability/porosity ratio. Tissue Eng. 2003; 9(3): 535–548.
24. Woodard JR, Hilldore AJ, Lan SK, Park CJ, Morgan AW, et al. The mechanical properties and osteoconductivity of hydroxyapatite bone scaffolds with multi-scale porosity. Biomater. 2007; 28: 45–54.
25. Deville S, Saiz E, Tomsia AP. Freeze casting of hydroxyapatite scaffolds for bone tissue engineering. Biomater. 2006; 27: 5480–5489.
26. Miranda P, Pajares A, Saiz E, Tomsia AP, Guiberteau F. Fracture modes under uniaxial compression in hydroxyapatite scaffolds fabricated by robocasting. J Biomed Mater Res. 2007; 83A: 646–655.
27. Ding M, Dalstra M, Danielsen CC, Kabel J, Hvid I, Linde F. Age variation in the properties of human tibial trabecular bone. J Bone Joint Surg. [Br] 1997; 79-B: 995–1002.
28. Ochia RS, Ching RP. Hydraulic resistance and permeability in human lumbar vertebral bodies. J Biomech Eng. 2002; 124: 533–537.
29. Gibson L. The mechanical behaviour of cancellous bone. J Biomech. 1985; 18(5): 317–328.
30. Røhl L, Larsen E, Linde F, Odgaard A, Jørgensen J. Tensile and compressive properties of cancellous bone. J Biomech. 1991; 24(12): 1143–1149.
31. Haddock SM, Debes JC, Nauman EA, Fong KE, Arramon YP, Keaveny TM. Structure-function relationships for coralline hydroxyapatite bone substitute. J Biomed Mater Res. 1999; 47(1): 71–78.
32. Kohles SS, Roberts J. Linear poroelastic cancellous bone anisotropy: trabecular solid elastic and fluid transport properties. J Biomech Eng-T. ASME 2002; 124(5): 521–526.
33. Sandino C, Kroliczek P, McErlain DD, Boyd SK. Predicting the permeability of trabecular bone by micro-computed tomography and finite element modeling. J Biomech. 2014; 47: 3129–3134.
34. Wagoner Johnson AJ, Herschler BA. A review of the mechanical behavior of CaP and CaP/polymer composites for applications in bone replacement and repair. Acta Biomater. 2011; 7(1): 16–30.
35. Drynda A, Hassel T, Bach FW, Peuster M. *In vitro* and *in vivo* corrosion properties of new iron-manganese alloys designed for cardiovascular applications. J Biomed Mater Res B. 2015; 103B: 649–660.
36. Kraus T, Moszner F, Fischerauer S, Fiedler M, Martinelli E, et al. Biodegradable Fe-based alloys for use in osteosynthesis: Outcome of an in vivo study after 52 weeks. Acta Biomater. 2014; 10: 3346–3353.
37. Zheng YF, Gu XN, Witte F. Biodegradable metals. Mater Sci Eng. 2014; R 77: 1–34.
38. Kamakura S, Sasano Y, Shimizu T, Hatori K, Suzuki O, Kagayama M, Motegi K. Implanted octacalcium phosphate is more resorbable than β-tricalcium phosphate and hydroxyapatite. J Biomed Mater Res. 2002; 59: 29–34.
39. Handschel J, Wiesmann HP, Stratmann U, Kleinheinz J, Meyer U, Joos U. TCP is hardly resorbed and not osteoconductive in a non-loading calvarial model. Biomater. 2002; 23: 1689–1695.

40. Kondo N, Ogose A, Tokunaga K, Ito T, Arai K, Kudo N, Inoue H, Irie H, Endo N. Bone formation and resorption of highly purified β-tricalcium phosphate in the rat femoral condyle. Biomater. 2005; 26: 5600–5608.
41. Teitelbaum SL. Bone resorption by osteoclasts. Science. 2000; 289: 1504–1508.
42. Barrère F, van Blitterswijk CA, de Groot K. Bone regeneration: molecular and cellular interactions with calcium phosphate ceramics. Int J Nanomedicine. 2006; 1: 317–332.
43. Zerbo IR, Bronckers ALJJ, de Lange G, Burger EH. Localisation of osteogenic and osteoclastic cells in porous β-tricalcium phosphate particles used for human maxillary sinus floor elevation. Biomater. 2005; 26: 1445–1451.
44. Minarelli Gaspar AM, Saska S, Carrodeguas RG, De Aza AH, Pena P, et al. Biological response to wollastonite doped α-tricalcium phosphate implants in hard and soft tissues in rats. Key Eng Mater. 2009; 396–398: 7–10.
45. Bose S, Tarafder S, Banerjee SS, Davies NM, Bandyopadhyay A. Understanding in vivo response and mechanical property variation in MgO, SrO and SiO_2 doped â-TCP. Bone. 2011; 48: 1282–1290.
46. Bandyopadhyay A, Petersen J, Fielding G, Banerjee S, Bose S. ZnO, SiO_2, and SrO doping in resorbable tricalcium phosphates: Influence on strength degradation, mechanical properties, and *in vitro* bone-cell material interactions. J Biomed Mater Res B. 2012; 100B: 2203–2212.